DOI: 10.17344/acsi.2019.5650 *Acta Chim. Slov.* **2020,** *67,* 644–650

Scientific paper

Synthesis, X-Ray Crystal Structure of Oxidovanadium(V) Complex Derived from 4-Bromo-*N*'-(2-hydroxybenzylidene) benzohydrazide with Catalytic Epoxidation Property

Qi-An Peng,[1] Xiang-Peng Tan,[1] Yi-Di Wang,[1] Si-Huan Wang,[1] You-Xin Jiang[1] and Yong-Ming Cui[1,2,3,*]

[1] *School of Environmental Engineering, Wuhan Textile University, Wuhan 430073, P. R. China*

[2] *National Local Joint Engineering Laboratory for Advanced Textile Processing and Clean Production, Wuhan Textile University, Wuhan 430073, P. R. China*

[3] *Hubei Provincial Engineering Laboratory for Clean Production and High Value Utilization of Bio-Based Textile Materials, Wuhan Textile University, Wuhan 430073, P. R. China*

** Corresponding author: E-mail: cuiym981248@163.com*

Received: 10-28-2019

Abstract

A new oxidovanadium(V) complex, [VOL(OCH_3)(CH_3OH)], where H_2L = 4-bromo-*N*'-(2-hydroxybenzylidene)benzohydrazide, has been synthesized and fully characterized on the basis of CHN elemental analysis, FT-IR, UV-Vis, ^1H and ^{13}C NMR spectroscopy. Structures of the free hydrazone and the complex were further characterized by single crystal X-ray diffraction, which indicates that the V atom in the complex adopts octahedral coordination, and the hydrazone ligand behaves as a tridentate ligand. The catalytic epoxidation property of the complex was investigated.

Keywords: Hydrazone; oxidovanadium complex; crystal structure; catalytic epoxidation

1. Introduction

Schiff bases are a kind of interesting ligands in coordination chemistry.[1] The metal complexes with Schiff bases have attracted remarkable attention due to their facile synthesis and special biological, catalytic and industrial applications.[2] Catalytic epoxidation of olefins is an important reaction in chemistry. Many transition metal complexes are active catalysts for this process.[3] However, among the complexes, vanadium and molybdenum complexes seem more interesting because of their excellent catalytic ability in the oxidation of olefins and sulfides.[4] In this paper, a new vanadium(V) complex derived from 4-bromo-*N*'-(2-hydroxybenzylidene)benzohydrazide (H_2L, Scheme 1) was prepared and studied for its catalytic epoxidation property on cyclooctene.

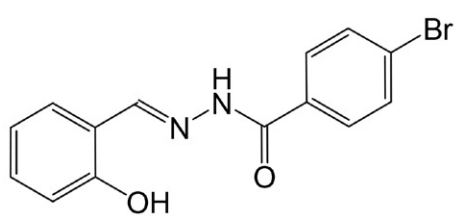

Scheme 1. The hydrazone H_2L.

2. Experimental

2. 1. Materials and Methods

4-Bromobenzohydrazide, salicylaldehyde and VO(acac)$_2$ were purchased from Alfa Aesar and used as received. Reagent grade solvents were used as received. Microanalyses of the complexes were performed with a Vario EL III CHNOS elemental analyzer. Infrared spectra were recorded as KBr pellets with an FTS-40 spectrophotometer. Electronic spectra were recorded on a Lambda 900 spectrometer. ^1H and ^{13}C NMR spectra were recorded on a Bruker spectrometer at 500 MHz. The catalytic reactions were followed by gas chromatography on an Agilent 6890A

chromatograph equipped with an FID detector and a DB5-MS capillary column (30 m × 0.32 mm, 0.25 μm). Molar conductance measurements were made by means of a Metrohm 712 conductometer in acetonitrile.

2. 2. Synthesis of 4-Bromo-*N*'-(2-Hydroxybenzylidene)benzohydrazide (H_2L)

4-Bromobenzohydrazide (10 mmol, 2.15 g) and salicylaldehyde (10 mmol, 1.22 g) were refluxed in methanol (50 mL). The reaction was continued for 1 h in oil bath during which a solid compound separated. It was filtered and washed with cold methanol. The crude product was recrystallized from methanol and dried over anhydrous $CaCl_2$. Yield: 2.36 g (74%). IR data (KBr pellet, cm^{-1}): 3445 ν(O–H), 3220 ν(N–H), 1643 ν(C=O), 1612 ν(C=N). UV-Vis data in methanol (nm): 287, 298, 327, 388. Analysis: Found: C 52.55, H 3.56, N 8.71%. Calculated for $C_{14}H_{11}BrN_2O_2$: C 52.69, H 3.47, N 8.78%. ^{1}H NMR (500 MHz, d^6-DMSO): δ 12.18 (s, 1H, O*H*), 11.22 (s, 1H, N*H*), 8.65 (s, 1H, C*H*=N), 7.90 (d, 2H, Ar*H*), 7.78 (d, 2H, Ar*H*), 7.57 (d, 1H, Ar*H*), 7.33 (t, 1H, Ar*H*), 6.93 (t, 2H, Ar*H*). ^{13}C NMR (126 MHz, d^6-DMSO) δ 162.72, 158.59, 143.07, 133.15, 130.79, 129.43, 129.39, 128.55, 128.49, 127.97, 127.69, 119.53, 118.15, 116.48.

2. 3. Synthesis of the Complex [VOL(OCH_3)(CH_3OH)]

The hydrazone compound H_2L (1.0 mmol, 0.32 g) and $VO(acac)_2$ (1.0 mmol, 0.26 g) were refluxed in methanol (30 mL). The reaction was continued for 1 h in oil bath to give a deep brown solution. Single crystals of the complex were formed during slow evaporation of the reaction mixture in air. The crystals were isolated by filtration, washed with cold methanol and dried over anhydrous $CaCl_2$. Yield: 0.23 g (51%). IR data (KBr pellet, cm^{-1}): 3438 ν(O–H), 1607 ν(C=N), 1390 ν(C–$O_{phenolate}$), 1157 ν(N–N), 953 ν(V=O). UV-Vis data in methanol (nm): 268, 323, 400. Molar conductance (10^{-3} mol L^{-1}, methanol): 27 Ω^{-1} cm^2 mol^{-1}. Analysis: Found: C 43.12, H 3.75, N 6.17%. Calculated for $C_{16}H_{16}BrN_2O_5V$: C 42.98, H 3.61, N 6.26%. ^{1}H NMR (500 MHz, d^6-DMSO): δ 13.93 (s, 1H, O*H*), 9.11 (s, 1H, C*H*=N), 7.78 (d, 1H, Ar*H*), 7.72 (t, 2H, Ar*H*), 7.58 (t, 1H, Ar*H*), 7.47 (t, 1H, Ar*H*), 7.42 (t, 1H, Ar*H*), 7.01 (t, 1H, Ar*H*), 6.90 (d, 1H, Ar*H*), 3.45 (s, 3H, CH_3), 2.12 (d, 3H, CH_3OH). ^{13}C NMR (126 MHz, d^6-DMSO) δ 167.40, 163.44, 156.14, 135.46, 133.70, 133.23, 132.25, 131.96, 131.11, 127.58, 120.87, 120.03, 119.07, 116.06, 40.02, 16.41.

2. 4. Crystal Structure Determination

Data were collected on a Bruker SMART 1000 CCD area diffractometer using a graphite monochromator Mo Kα radiation (λ = 0.71073 Å) at 298(2) K. The data were corrected with SADABS programs and refined on F^2 with Siemens SHELXL software.[5] The structures of H_2L and the complex were solved by direct methods and difference Fourier syntheses. All non-hydrogen atoms were refined anisotropically. The amino H atom (H2) in H_2L and the methanol H atom (H5) in the complex were located from difference Fourier maps and refined isotropically. The remaining hydrogen atoms were placed in calculated positions and included in the last cycles of refinement. Crystal data and details of the data collection and refinement are listed in Table 1.

Table 1. Crystallographic Data for H_2L and the Complex

Parameters	H_2L	The complex
Empirical formula	$C_{14}H_{11}BrN_2O_2$	$C_{16}H_{16}BrN_2O_5V$
Formula weight	319.16	447.16
Crystal system	Monoclinic	Triclinic
Space group	$P2_1/n$	P –1
a [Å]	5.9246(9)	7.7967(11)
b [Å]	29.6219(12)	11.1240(13)
c [Å]	7.5728(11)	11.6316(12)
α [°]	90	66.901(1)
β [°]	92.303(1)	83.748(1)
γ [°]	90	71.652(1)
V [Å^3]	1327.9(3)	880.6(2)
Z	4	2
$\rho_{calcd.}$ [g cm^{-3}]	1.596	1.686
μ [mm^{-1}]	3.094	2.861
F(000)	640	448
Measured reflections	7903	5279
Independent reflections	2468	3274
Observed reflections ($I > 2\sigma(I)$)	1661	1677
Parameters	176	229
Restraints	1	1
Final R indices [$I > 2\sigma(I)$]	0.0384, 0.0729	0.0581, 0.0856
R indices (all data)	0.0732, 0.0845	0.1438, 0.1140
Goodness-of-fit on F^2	1.013	1.005
Largest difference in peak and hole (e Å^{-3})	0.266 and –0.207	0.422 and –0.463

2. 5. Catalytic Epoxidation Process

A mixture of cyclooctene (2.76 mL, 20 mmol), acetophenone (internal reference) and the complex as the catalyst (0.05 mmol) was stirred and heated up to 80 °C before addition of aqueous *tert*-butyl hydroperoxide (TBHP; 70% w/w, 5.48 mL, 40 mmol). The mixture is initially an emulsion, but two phases become clearly visible as the reaction progresses, a colorless aqueous one and a yellowish organic one. The reaction was monitored for 5 h with withdrawal and analysis of organic phase aliquots (0.1 mL) at required times. Each withdrawn sample was mixed with 2 mL of diethylether, treated with a small quantity of MnO_2 and then filtered through silica and analyzed by GC.

3. Results and Discussion

3. 1. Synthesis

The hydrazone compound H_2L and the complex were synthesized in a facile and analogous way (Scheme 2).

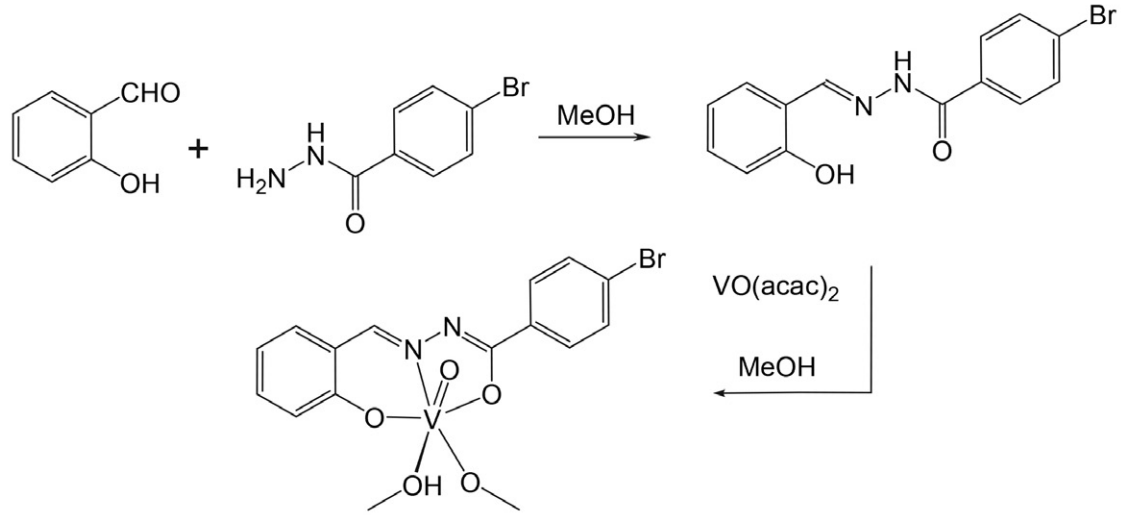

Scheme 2. The synthesis of the hydrazone H_2L and the complex

The hydrazone H_2L acts as a tridentate dianionic ONO donor ligands toward the VO^{2+} core. The vanadium complex was obtained from a refluxing mixture of the hydrazone and $VO(acac)_2$ in 1:1 molar proportion in methanol. The complex was isolated as brown single crystals from the reaction mixture by slow evaporation at room temperature. Crystals of the complex are stable at room temperature and are found to be fairly soluble in most of the common organic solvents such as methanol, ethanol, acetonitrile, DMF and DMSO. The low molar solution conductance of the complex in methanol indicates its non-electrolyte behavior.

3. 2. IR and Electronic Spectra

The IR spectrum of the hydrazone H_2L shows bands centered at 3220 cm^{-1} for ν(N–H), 3445 cm^{-1} for ν(O–H), and 1643 cm^{-1} for ν(C=O).[6] The peaks attributed to ν(N–H) and ν(C=O) are absent in the spectrum of the complex as the ligand binds in dianionic form resulting in losing proton from carbohydrazide group. Strong band observed at 1607 cm^{-1} for the complex is attributed to ν(C=N), which is located at lower frequencies as compared to the free hydrazone ligand, *viz.* 1612 cm^{-1}.[7] The complex exhibits characteristic band at 953 cm^{-1} for the stretching of V=O bond.[8] Based on the IR absorption, it is obvious that the hydrazone ligand exists in the uncoordinated form in *keto*-amino tautomer form and in the complex in imino-enol tautomeric form. This is not uncommon in the coordination of the hydrazone compounds.[9]

Electronic spectrum of the complex recorded in methanol displays strong absorption band centered at 400 nm, which is assigned as charge transfer transitions of N($p\pi$)–Mo($d\pi$) LMCT. The medium absorption band centered at 323 nm for the complex is assigned as charge transfer transitions of O($p\pi$)–Mo($d\pi$) LMCT.[10]

3. 3. Description of the Structure of H_2L

The perspective view of H_2L together with the atom numbering scheme is shown in Figure 1. Selected bond lengths and angles are given in Table 2. The molecule adopts an *E* configuration with respect to the methylidene unit. The methylidene bond, with the distance of 1.264(4) Å, confirms it a typical double bond. The shorter distance of the C8–N2 bond (1.343(4) Å) and the longer distance of the C8–O2 bond (1.225(4) Å) for the amide group than usual, suggests the presence of conjugation effects in the hydrazone molecule. The presence of intramolecular O1–H1···N1 hydrogen bond, as well as the conjugation effects, result in the two benzene rings form a dihedral angle of 6.8(5)°. In the crystal structure of the compound, the hydrazone molecules are linked by intermolecular

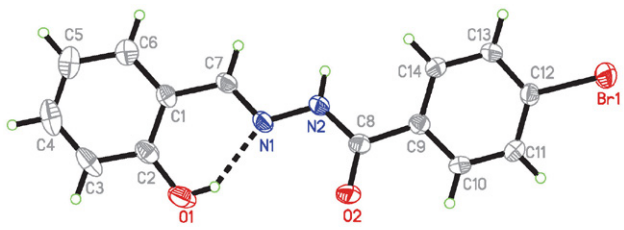

Figure 1. ORTEP plots (30% probability level) and numbering scheme for H_2L.

Table 2. Selected Bond Lengths (Å) and Angles (°) for H_2L and the Complex

H2L			
C7–N1	1.264(4)	N1–N2	1.386(3)
C8–N2	1.343(4)	C8–O2	1.225(4)
Complex			
V1–O1	1.849(4)	V1–O2	1.948(4)
V1–O3	1.582(4)	V1–O4	1.757(4)
V1–O5	2.358(5)	V1–N1	2.119(5)
O3–V1–O4	103.4(2)	O3–V1–O1	99.7(2)
O4–V1–O1	101.1(2)	O3–V1–O2	96.2(2)
O4–V1–O2	94.8(2)	O1–V1–O2	154.2(2)
O3–V1–N1	97.0(2)	O4–V1–N1	157.9(2)
O1–V1–N1	83.5(2)	O2–V1–N1	74.5(2)
O3–V1–O5	173.7(2)	O4–V1–O5	81.3(2)
O1–V1–O5	83.3(2)	O2–V1–O5	79.0(2)
N1–V1–O5	77.7(2)		

Table 3 Hydrogen bond distances (Å) and bond angles (°) for H_2L and the complex

D*–H···*A	***d*(*D*–H)**	***d*(H···*A*)**	***d*(*D*···*A*)**	**Angle (*D*–H···*A*)**
H_2L				
O1–H1···N1	0.82	1.92	2.627(3)	144(5)
N2–H2···O2^{i}	0.90(1)	1.97(1)	2.851(3)	168(3)
C7–H7···O2^{i}	0.93	2.55(2)	3.261(3)	134(3)
Complex				
O5–H5···N2^{ii}	0.85(1)	2.01(2)	2.828(6)	163(7)

Symmetry codes: (i) –½ + x, ½ – y, –½ + z; (ii) – x, 1 – y, 1 – z.

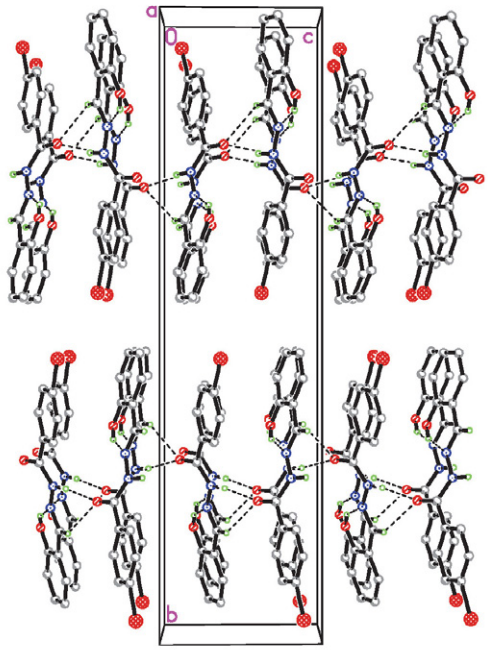

Figure 2. The molecular packing diagram of H_2L, viewed down the *a* axis. Hydrogen bonds are shown as dashed lines.

N2–H2···O2 and C7–H7···O2 hydrogen bonds, to form 1D chains running along the *c* axis (Table 3, Figure 2).

3. 4. Description of the Structure of the Complex

The perspective view of the complex together with the atom numbering scheme is shown in Figure 3. The coordination geometry around the V atom reveals a distorted octahedral environment with NO_5 chromophore. The hydrazone ligand behaves as a dianionic tridentate ligand binding through the phenolate oxygen, the enolate oxygen and the imine nitrogen, and occupies three positions in the equatorial plane. The fourth position of the equatorial plane is occupied by the deprotonated methanol ligand. The neutral methanol ligand occupies one axial position of the octahedral coordination, and the other axial position is defined by the oxido group. The vanadium atom is found to be deviated from the mean equatorial planes defined by the four donor atoms by 0.310(2) Å. The V1–O5 bond length is longer than the normal single bond lengths (2.358(5) Å against 1.9–2.0 Å). This shows that the neutral methanol ligand is loosely attached to the V center. This is due to the *trans* effect generated by the oxido group. The remaining V–O bond lengths of 1.58–1.95 Å and the V–N bond length of 2.12 Å are similar to the corresponding bond values observed in other vanadium(V) complexes.[11] The C8–O2 bond length in the complex is 1.311(7) Å, which is closer to single bond length rather than C=O double bond length. However, the shorter length compared to C–O single bond may be attributed to extended electron delocalization in the ligand.[12] Similarly shortening of C8–N2 bond length (1.308(7) Å instead of normal 1.38 Å) together with the elongation of N1–N2 bond length (1.398(6) Å) also supports the electron cloud delocalization in the ligand system. The hydrazone ligand forms a five-membered and a six-membered chelate rings with the V center. The five-membered metallacycle ring is thus rather planar, but the six-membered metallacycle ring is clearly distorted. The two benzene rings form a dihedral angle of 4.3(5)°. The *trans* angles are in the range 154.2(2)–173.7(2)°, indicating considerable

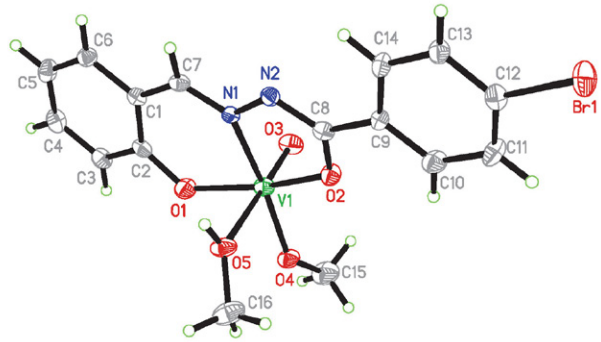

Figure 3. ORTEP plots (30% probability level) and numbering scheme for the complex.

distortion of the coordination octahedron around the V center.

In the crystal structure of the complex, adjacent two complex molecules are linked by intermolecular O5–H5···N2 hydrogen bonds (Table 3), to form dimers (Table 3, Figure 4).

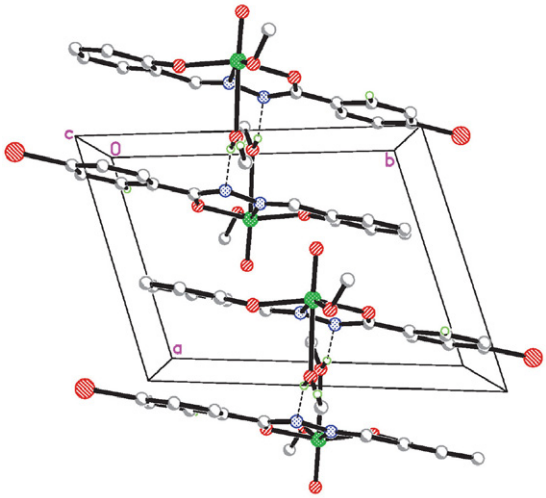

Figure 4. The molecular packing diagram of the complex, viewed down the *c* axis. Hydrogen bonds are shown as dashed lines.

3. 5. Catalytic Epoxidation Results

Before addition of aqueous TBHP at 80 °C, the complex dissolved completely in the organic phase. The aqueous phase of the solution was colorless and the organic phase was brown, indicating that the catalyst is mainly confined in the organic phase. TBHP is mainly transferred into the organic phase under those conditions, and for that reason the reactant and products in the organic layer were analyzed. Cyclooctene and cyclooctene oxide are not significantly soluble in water, therefore the determination of the epoxide selectivity (epoxide formation/cyclooctene conversion) is expected to be accurate. For the cyclooctene epoxidation by using aqueous TBHP, with no extra addition of organic solvents, the present study shows effective activity. Kinetic profiles of the complex as catalyst are presented in Figure 5. No induction time was observed. The cyclooctene conversion for the complex is 93% after 5 h, and the selectivity towards cyclooctene oxide is 67%. Possible mechanistic consideration involves coordination of TBHP as a neutral molecule, with the hydrogen bond O–H···O (Scheme 3).

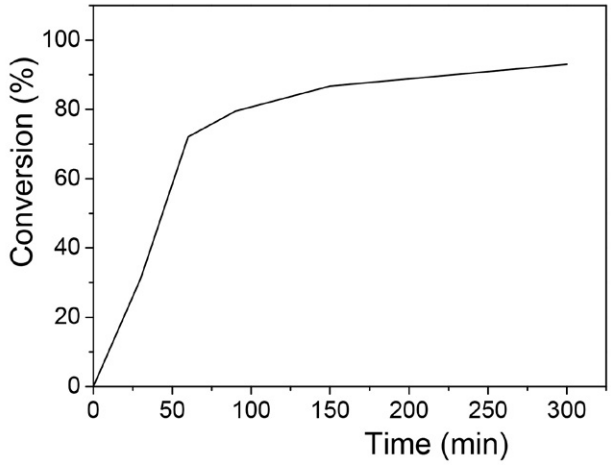

Figure 5. Kinetic monitoring of *cis*-cyclooctene epoxidation with TBHP–H_2O in the presence of the complex.

4. Conclusion

In summary, a new hydrazone compound 4-bromo-*N*'-(2-hydroxybenzylidene)benzohydrazide was prepared and structurally characterized. With the hydrazone

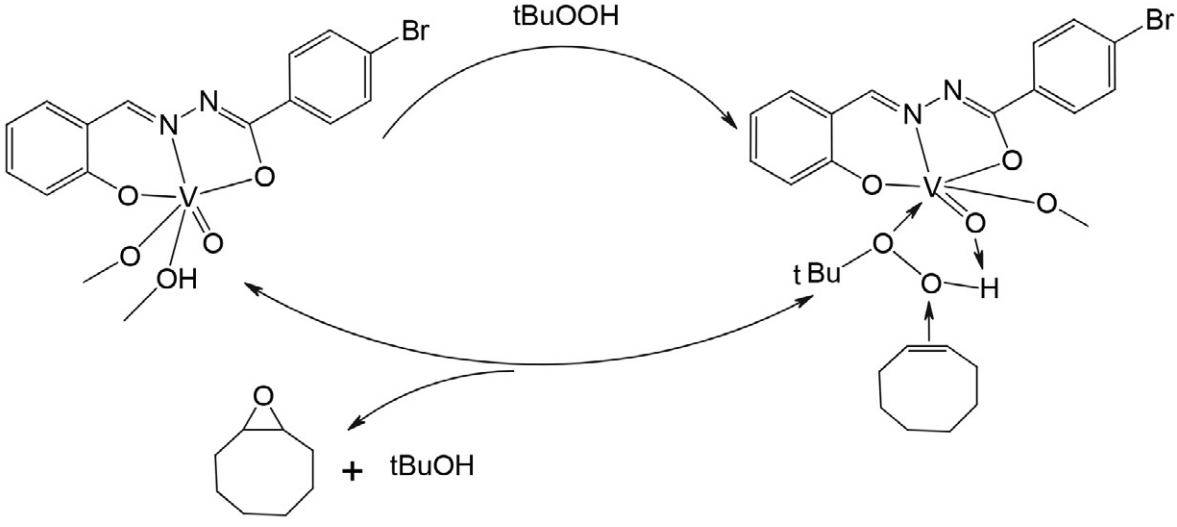

Scheme 3. Proposed mechanism for the catalytic process of the complex.

compound, a new oxidovanadium(V) complex was synthesized and characterized. Single crystal structures of the hydrazone compound and the oxidovanadium(V) complex were determined. The hydrazone compound coordinate to the V atom through the NNO donor set. The V atom of the complex is in octahedral coordination. The complex can catalyze the epoxidation of cyclooctene, with high conversion and selectivity.

5. Supplementary Data

CCDC numbers 1916011 for H_2L and 1916013 for the complex contain the supplementary crystallographic data. These data can be obtained free of charge *via* http://www.ccdc.cam.ac.uk/conts/retrieving.html, or from the Cambridge Crystallographic Data Center, 12, Union Road, Cambridge CB2 1EZ, UK; fax: +44 1223 336 033; or e-mail: deposit@ccdc.cam.ac.uk.

Acknowledgments

This work was supported by the Collaborative Innovation Plan of Hubei Province for Key Technology of Eco-Ramie Industry.

6. References

1. (a) R. Dhiman, C. M. Nagaraja, *New J. Chem.* **2019**, *43*, 13662–13669; **DOI:**10.1039/C9NJ02281C
(b) J. E. Baumeister, A. W. Mitchell, S. P. Kelley, C. L. Barnes, S. S. Jurisson, *Dalton Trans.* **2019**, *48*, 12943–12955; **DOI:**10.1039/C9DT02630D
(c) A. Najafian, T. R. Cundari, *Inorg. Chem.* **2019**, *58*, 12254–12263; **DOI:**10.1021/acs.inorgchem.9b01696
(d) H.-Y. Qian, N. Sun, *Transition Met. Chem.* **2019**, *44*, 501–506; **DOI:**10.1007/s11243-018-00296-x
(e) L. Pogany, B. Brachnakova, P. Masarova, J. Moncol, J. Pavlik, M. Gal, M. Mazur, R. Herchel, I. Nemec, I. Salitros, *New J. Chem.* **2019**, *43*, 13916–13928; **DOI:**10.1039/C9NJ03087E
(f) H.-Y. Qian, *Inorg. Nano-Met. Chem.* **2018**, *48*, 615–619. **DOI:**10.1080/24701556.2019.1567542
2. (a) R. Ogawa, T. Suzuki, M. Hirotsu, N. Nishi, Y. Shimizu, Y. Sunatsuki, Y. Teki, I. Kinoshita, *Dalton Trans.* **2019**, *48*, 13622–13629; **DOI:**10.1039/C9DT03007G
(b) H.-Y. Qian, *Inorg. Nano-Met. Chem.* **2018**, *48*, 461–466; **DOI:**10.1080/24701556.2019.1569689
(c) H. Y. Qian, *Russ. J. Coord. Chem.* **2017**, *43*, 780–786; **DOI:**10.1134/S1070328417110070
(d) I. Mondal, K. Ghosh, S. Chattopadhyay, *Inorg. Chim. Acta* **2019**, *494*, 123–131; **DOI:**10.1016/j.ica.2019.05.003
(e) M. H. Esfahani, H. Iranmanesh, J. E. Beves, M. Kaur, J. P. Jasinski, M. Behzad, *J. Coord. Chem.* **2019**, *72*, 2326–2336; **DOI:**10.1080/00958972.2019.1643846
(f) H. Y. Qian, *Russ. J. Coord. Chem.* **2018**, *44*, 32–38. **DOI:**10.1134/S1070328418010074
3. (a) L. S. Neira, M. M. Antunes, A. C. Gomes, L. Cunha-Silva, M. Pillinger, A. D. Lopes, A. A. Valente, I. S. Goncalves, *Dalton Trans.* **2019**, *48*, 11508–11519; **DOI:**10.1039/C9DT02127B
(b) H. Albright, P. S. Riehl, C. C. McAtee, J. P. Reid, J. R. Ludwig, L. A. Karp, P. M. Zimmerman, M. S. Sigman, C. S. Schindler, *J. Am. Chem. Soc.* **2019**, *141*, 1690–1700. **DOI:**10.1021/jacs.8b11840
4. (a) G. Romanowski, J. Kira, M. Wera, *Polyhedron* **2014**, *67*, 529–539; **DOI:**10.1016/j.poly.2013.10.008
(b) J.-Q. Wu, Y.-S. Li, *Coord. Chem. Rev.* **2011**, *255*, 2303–2314; **DOI:**10.1016/j.ccr.2011.01.048
(c) K. Nomura, S. Zhang, *Chem. Rev.* **2011**, *111*, 2342–2362; **DOI:**10.1021/cr100207h
(d) A. V. Chuchuryukin, R. B. Huang, E. E. van Faassen, G. P. M. van Klink, M. Lutz, J. C. Chadwick, A. L. Spek, G. van Koten, *Dalton Trans.* **2011**, *40*, 8887–8895; **DOI:**10.1039/c1dt10482a
(e) M. L. Kuznetsov, J. C. Pessoa, *Dalton Trans.* **2009**, *28*, 5460–5468; **DOI:**10.1039/b902424g
(f) X.-W. Zhu, *Acta Chim. Slov.* **2018**, *65*, 939–945; **DOI:**10.17344/acsi.2018.4607
(g) M. Liang, N. Sun, D.-H. Zou, *Acta Chim. Slov.* **2018**, *65*, 964–969; **DOI:**10.17344/acsi.2018.4625
(h) L.-W. Xue, Q.-L. Peng, P.-P. Wang, H.-J. Zhang, *Acta Chim. Slov.* **2019**, *66*, 694–700. **DOI:**10.17344/acsi.2019.5151
5. G. M. Sheldrick, SHELXS97 Program for solution of crystal structures, University of Göttingen, Germany, **1997**.
6. (a) Y.-T. Ye, F. Niu, Y. Sun, D. Qu, X.-L. Zhao, J. Wang, D.-M. Xian, H. Jurg, Z.-L. You, *Chinese J. Inorg. Chem.* **2015**, *31*, 1019–1026;
(b) Z.-L. You, D.-M. Xian, M. Zhang, *CrystEngComm* **2012**, *14*, 7133–7136. **DOI:**10.1039/c2ce26201k
7. (a) R. A. Lal, M. Chakrabarty, S. Choudhury, A. Ahmed, R. Borthakur, A. Kumar, *J. Coord. Chem.* **2010**, *63*, 163–175; **DOI:**10.1080/00958970903259451
(b) T. Glowiak, L. Jerzykiewicz, J. A. Sobczak, J. J. Ziolkowski, *Inorg. Chim. Acta* **2003**, *356*, 387–392. **DOI:**10.1016/S0020-1693(03)00301-3
8. C. A. Koellner, N. A. Piro, W. S. Kassel, C. R. Goldsmith, C. R. Graves, *Inorg. Chem.* **2015**, *54*, 7139–7141. **DOI:**10.1021/acs.inorgchem.5b01136
9. (a) L.-X. Li, Y. Sun, Q. Xie, Y.-B. Sun, K.-H. Li, W. Li, Z.-L. You, *Chinese J. Inorg. Chem.* **2016**, *32*, 369–376;
(b) L. Pan, C. Wang, K. Yan, K.-D. Zhao, G.-H. Sheng, H.-L. Zhu, X.-L. Zhao, D. Qu, F. Niu, Z.-L. You, *J. Inorg. Biochem.* **2016**, *159*, 22–28; **DOI:**10.1016/j.jinorgbio.2016.02.017
(c) D. Qu, F. Niu, X. Zhao, K.-X. Yan, Y.-T. Ye, J. Wang, M. Zhang, Z. You, *Bioorg. Med. Chem.* **2015**, *23*, 1944–1949. **DOI:**10.1016/j.bmc.2015.03.036
10. (a) R. Hahn, U. Kusthardt, W. Scherer, *Inorg. Chim. Acta* **1993**, *210*, 177–182; **DOI:**10.1016/S0020-1693(00)83325-3
(b) S. Gupta, A. K. Barik, S. Pal, A. Hazra, S. Roy, R. J. Butcher, S. K. Kar, *Polyhedron* **2007**, *26*, 133–141. **DOI:**10.1016/j.poly.2006.08.001

11. (a) M. R. Maurya, S. Agarwal, C. Bader, M. Ebel, D. Rehder, *Dalton Trans.* **2005**, 537-544;
(b) H.-Y. Qian, *Acta Chim. Slov.* **2019**, *66*, 995–1001.
DOI:10.4149/neo_2019_190112N36

12. H. H. Monfared, S. Alavi, R. Bikas, M. Vahedpour, P. Mayer, *Polyhedron* **2010**, *29*, 3355–3362.
DOI:10.1016/j.poly.2010.09.029

Povzetek

Sintetizirali smo nov oksidovanadijev(V) kompleks, [VOL(OCH_3)(CH_3OH)], kjer je H_2L = 4-bromo-*N*'-(2-hidroksibenziliden)benzohidrazid, in ga okarakterizirali z CHN elementno analizo, FT-IR, UV-Vis, ^1H in ^{13}C NMR spektroskopijo. Strukturi prostega hidrazona in kompleksa smo okarakterizirali tudi z monokristalno rentgensko difrakcijo, ki je razkrila, da ima V atom oktaedrično koordinacijo ter da je hidrazon trovezni ligand. Raziskali smo tudi katalitične lastnosti pri epoksidaciji.